International Compressor Engineering Conference   School of Mechanical Engineering

2008

Modeling and Testing of a Two-Stage Rotary Compressor

Margaret M. Mathison
Purdue University

James E. Braun
Purdue University

Eckhard A. Groll
Purdue University

Follow this and additional works at: https://docs.lib.purdue.edu/icec

Modeling and Testing of a Two-Stage Rotary Compressor

Margaret M. MATHISON*, James E. BRAUN, Eckhard A. GROLL

[1]Purdue University, School of Mechanical Engineering,
West Lafayette, Indiana, USA

*Corresponding Author: 765-490-5856 (phone), 765-494-0787 (fax), mmathiso@purdue.edu

ABSTRACT

While previous research studies have analyzed the compression process of single-stage rotary compressors, little information is available on two-stage rotary compressors. However, two-stage compressors provide opportunities for energy savings through modifications such as intercooling and economizing. This paper presents a computer model of a hermetic two-stage rotary compressor that was developed to provide design engineers with the means to optimize the compressor design.

The computer model considers the effects of leakages and heat transfer in its calculations to estimate the compressor power input and refrigerant mass flow rate. The model can be operated both with and without intercooling between the stages. External measurements were conducted using a prototype compressor to validate the model. The intermediate temperature and pressure, discharge temperature, power consumption, and mass flow rate were recorded for seventeen different operating conditions. The model predicts the compressor power consumption and mass flow rate within ±5% of the experimental results.

1. INTRODUCTION

Previous researchers have analyzed the compression process of single-stage rolling-piston compressors. Several researchers have focused on providing a detailed analysis of the compression chamber geometry and the motion of the rolling piston in the cylinder (Okada and Kuyama, 1982; Yanagisawa *et al.*, 1982). While some papers explore force balances and frictional losses in rolling piston compressors in detail, this project assumed a constant mechanical efficiency, eliminating the need for a force analysis.

Another topic that many researchers have explored is the refrigerant and oil leakage that occurs in rolling-piston compressors. Yanagisawa and Shimizu focused on the leakage through the radial clearance between the roller and the cylinder (1985a), and leakage across the roller face (1985b). Lee and Min (1988) combined a study of leakage losses and frictional losses to better understand sources of inefficiencies in the compressor. Heat transfer from the cylinder to the refrigerant gas is also a significant source of inefficiencies in the compressor. However, no new correlations have been developed to characterize the heat transfer in a rolling piston chamber, so researchers have proposed different methods of modeling this process. Shimizu *et al.* (1980) suggested using Dittus and Boelter's formula for the heat transfer coefficient, while Padhy and Dwivedi (1994) used a correlation for reciprocating compressors in the compression chamber. The correlation selected for this project, originally developed for spiral plate tube heat exchangers, was demonstrated for a scroll compressor by Chen *et al.* (2002a).

Though several researchers have combined the topics of friction, leakage and heat transfer losses to develop models for single-stage rolling piston compressors, analysis of two-stage compressors is limited. Mechanical friction losses have been considered (Jun, 2002), but no analysis pulls together the friction, leakage, and heat transfer losses for a two-stage model. Because of the potential for energy savings through intercooling or economizing between stages, the development of a two-stage model that can consider these different system configurations is important. As the demand for energy efficient air conditioning and refrigeration equipment increases and companies seek to incorporate two-stage compressors into systems, engineers will need models that can be used to develop optimized two-stage compressor designs.

The current paper presents a complete model for a hermetic two-stage rotary compressor. Results from the simulation model are compared to external compressor measurements, which were conducted using an available

compressor load stand (Chen *et al.*, 2002b). The model was also used to study the performance of the existing compressor in order to understand the relative importance of different leakage paths and the impact of intercooling on performance.

2. MODELING EQUATIONS

2.1 Geometry of the Chambers

The geometry of the rolling piston and cylinder is shown in Figure 1. In this diagram the roller is drawn to follow a counterclockwise path, with the suction port located to the left of the vane and the discharge port to the right of the vane. The crankshaft angle, θ, is defined as the angle between the vane slot and the point of contact between the rolling piston and the cylinder wall. The angle is measured across the suction chamber. While the beginning of the crankshaft revolution, when the compression chamber volume is at a maximum, corresponds to an angle of 0° for both stages, it is important to note that the two stages are 180° out of phase. This must be taken into consideration when linking the two stages in the model

The volume of the compression chamber can be calculated using the known dimensions of the compressor and the calculated vane extension. These calculations have been described by previous authors,
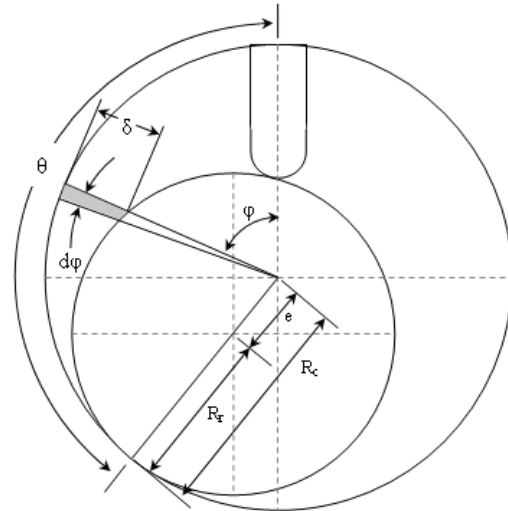
Figure 1. Compressor geometry.

such as Okada and Kuyama (1982). The surface area of the suction and compression chambers must also be calculated for use in the heat transfer calculations. Figure 1 shows a variable δ defined to measure the distance between the cylinder wall and the roller at any angle φ. This distance is both a function of the crankshaft angle, θ, and the angle at which it is measured, φ:

$$\delta = R_c - \frac{2e\cos(\theta-\varphi)\pm\sqrt{4e^2\cos^2(\theta-\varphi)-4\left(e^2-R_r^{\,2}\right)}}{2} \tag{1}$$

The area of the chamber on the top and bottom of the cylinder is then calculated by numerically integrating the distance between the cylinder wall and the roller across the entire chamber. This area is then added to the area of the vertical surfaces to determine the total surface area of each chamber.

2.2 Chamber Conservation of Mass

A mass balance can be written for the gas within the suction and compression chambers, mufflers, and upper and lower cavities of the shell as follows,

$$\frac{d(\rho V)}{dt} = \sum \dot{m}_{in} - \sum \dot{m}_{out} \tag{2}$$

By application of the chain rule for differentiation, and assuming that density is a function of temperature and pressure, the mass balance can be rewritten in terms of the unknowns dP/dθ and dT/dθ:

$$V\left(\frac{\delta\rho}{\delta P}\frac{dP}{d\theta}+\frac{\delta\rho}{\delta T}\frac{dT}{d\theta}\right) = -\rho\frac{dV}{d\theta}+\left(\sum \dot{m}_{in}-\sum \dot{m}_{out}\right)\frac{1}{\omega} \tag{3}$$

2.3 Chamber Conservation of Energy

An energy balance for the gas in the suction and compression chambers, mufflers, and upper and lower cavities of the shell can be written as follows:

$$\frac{dE_{cv}}{dt} = \sum \dot{m}_{in}h_{in} - \sum \dot{m}_{out}h_{out} + \dot{Q} - \dot{W} \tag{4}$$

The enthalpy terms in the energy balance account for the energy transfer by gas flow through the suction pipe, discharge pipe, and leakage paths. Assuming that the compression process is a quasi-equilibrium process, the

changes in kinetic and potential energy are negligible, and the specific internal energy is a function of pressure and temperature, the energy balance can be rewritten as,

$$\left(uV\frac{\delta\rho}{\delta P}+\rho V\frac{\delta u}{\delta P}\right)\frac{dP}{d\theta}+\left(uV\frac{\delta\rho}{\delta T}+\rho V\frac{\delta u}{\delta T}\right)\frac{dT}{d\theta}=-\left(u\rho+P\right)\frac{dV}{d\theta}+\left(\sum\dot{m}_{in}h_{in}-\sum\dot{m}_{out}h_{out}+\dot{Q}\right)\frac{1}{\omega} \qquad (5)$$

2.4 Chamber Leakage Model

Leakage occurs to and from the suction and compression chambers and the upper and lower cavities of the compressor at several locations, causing an overall decrease in efficiency due to the re-expansion of compressed gas. Figure 2 shows a sketch of a single stage of the compressor with the flow paths marked by arrows, including leakage, inlet, and outlet flows. The types of flows are classified as either isentropic flow of compressible ideal gas, laminar viscous flow, or mixed plane Couette and Poiseuille flow. The isentropic flow model is used for leakage paths dominated by pressure driven flow, while mixed Couette and Poiseuille flows models are used for leakages driven by both pressure differences and wall motion. The laminar viscous flow model is applied to paths with high concentrations of lubrication. More detailed descriptions of these three flow models can be found in basic fluid dynamics textbooks (Munson *et al.*, 2002).
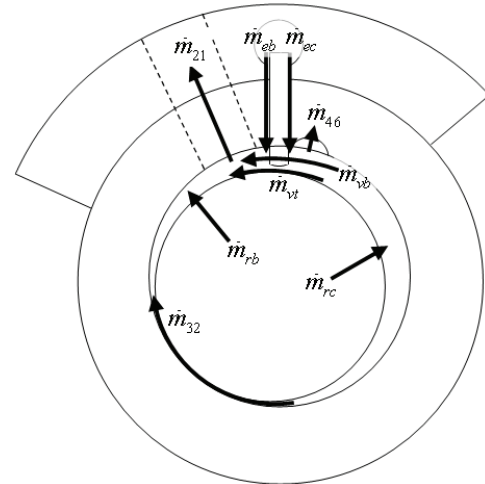
Figure 2. Schematic of leakage paths in the compression cylinder.

2.5 Valve Model

The motion of the valve is predicted using the pressure difference between the compression chamber and the muffler to predict the valve's acceleration. The acceleration of the valve at any point in time $t + \Delta t$ depends on its displacement, y_n, and velocity, y_n', at time t:

$$y_{n+1}'' = a - by_n' - cy_n \qquad (6)$$

where coefficients a, b, and c depend on the maximum displacement of the valve, the mass of the valve, and the diameter of the discharge port, D_{dp}, which are all known properties of the compressor. They also depend on a friction factor, a damping coefficient, and a spring constant that must be determined experimentally. The valve position can then be determined numerically and used to calculate an effective cross-sectional area for the mass flow through the valve. Finally, the isentropic flow model is applied to calculate the mass flow rate based on the pressure across the discharge port and the effective cross-sectional area.

2.6 Heat Transfer Model

Heat transfer between the cylinder wall and the gas in the suction and compression chambers is calculated by determining an appropriate convection coefficient and applying Newton's law of cooling. The spiral heat exchanger model that has been applied to scroll compressors (Chen *et al.*, 2002a; Yi *et al.*, 2004) was selected for modeling the heat exchange in the rolling piston suction and compression chambers. The spiral heat exchanger model relates the heat transfer coefficient to the Reynolds number, *Re*, and Prandtl number, *Pr*, by the expression

$$h_c=0.023\frac{k}{D_h}\mathrm{Re}^{0.8}\,\mathrm{Pr}^4\left[1.0+1.77\left(\frac{D_h}{r_{aver}}\right)\right] \qquad (7)$$

where D_h is the hydraulic diameter and r_{aver} is the average radius of the chamber. The gas velocity used to calculate the Reynolds number was approximated as the average surface velocity of the cylinder and the roller.

Newton's law of cooling also applies to the heat transfer from the outer surface of the compression cylinder to the gas in the shell. However, for this case the correlation for forced convection in an annulus is used to predict the heat transfer coefficient. The heat transfer rates from both the interior and exterior walls of the cylinder depend on the cylinder temperature. For these calculations, the temperature of the cylinder surface is assumed to have a linear distribution around the cylinder, varying from 5 K above the average cylinder temperature near the discharge port to 5 K below the average cylinder temperature near the suction port. However, since the average cylinder temperature is initially unknown, solving for the heat transfer is an iterative process.

2.7 Intercooling Model

When intercooling is incorporated, the model uses a specified degree of superheat at the second stage suction to control the amount of intercooling. The model calculates the saturation temperature corresponding to the pressure in the first stage muffler and adds the specified superheat to determine the temperature of the gas available to the second stage. The required capacity of the intercooler to achieve the specified superheat, Q_{int}, is determined by multiplying the change in the enthalpy of the fluid across the intercooler, Δh_{int}, by its mass flow rate:

$$\dot{Q}_{int} = \dot{m}\Delta h_{int} \qquad (8)$$

2.8 Shell Energy Balance

A simple shell energy balance is applied to the compressor to estimate the temperature of the gas in the shell. For these calculations it is assumed that all of the compressor power lost due to mechanical and electrical inefficiencies is transferred to the gas in the shell as heat. It is also assumed that the outer surface of the compressor is at the same temperature as the gas in the shell. Therefore, according to Newton's law of cooling, the amount of heat lost to the environment is proportional to the difference between the shell and ambient gas temperatures and the heat transfer coefficient for natural convection from a vertical cylinder. However, solving the shell energy balance for the shell temperature is an iterative process because both the enthalpy of the gas leaving the shell and the rate of heat transfer from the shell due to natural convection depend on the shell temperature.

3. NUMERICAL SOLUTION OF THE MODEL

For each control volume, the mass and energy balance equations can be solved simultaneously for the differential temperature and pressure using Cramer's Rule. The modified Euler method can then be used to solve for the temperatures and pressures in the control volumes over an entire crankshaft revolution. After the mass and energy balance is applied to the first stage suction chamber and the first stage compression chamber, the mass flow rate into the first stage is compared to the mass flow rate exiting the first stage. The temperature in the first stage muffler, assumed to be constant over each revolution, is then adjusted to satisfy the first stage mass balance. Without changing the first stage muffler pressure, also assumed to be constant, the model continues to loop through the first stage calculations until the first stage inlet and outlet mass flow rates agree within a specified tolerance. This fixes the first stage muffler temperature.

The model then repeats the process for the second stage. The second stage muffler pressure is held constant at the discharge pressure while the second stage muffler temperature is varied to satisfy the second stage mass balance.

The temperature of the gas in the shell is determined based on the shell energy balance. Because leakage occurs from
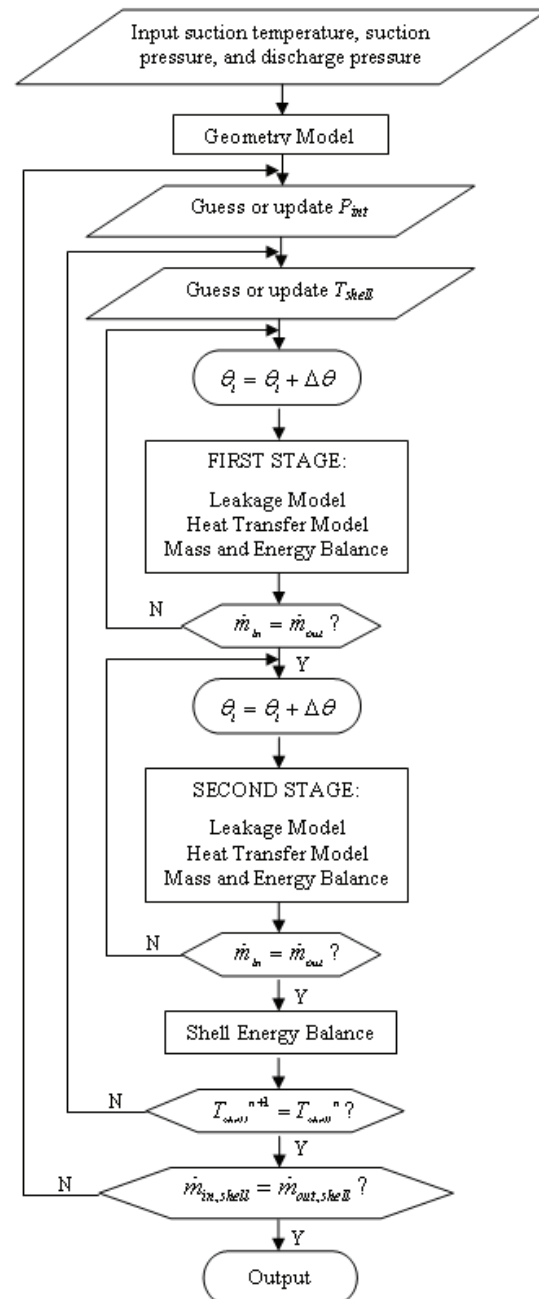
Figure 3. Flow chart of two-stage rolling piston compressor model.
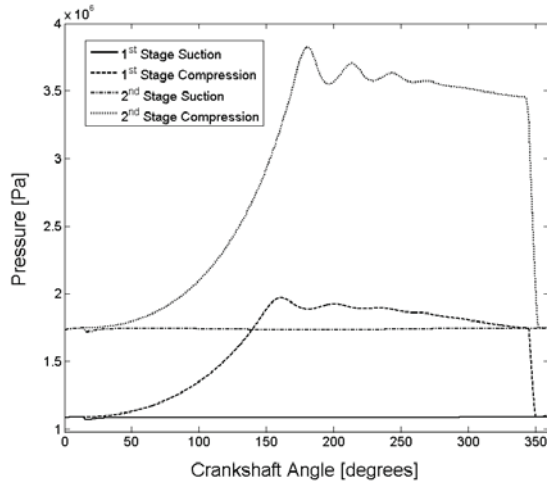
Figure 4. Variation of pressure with crankshaft angle predicted at Test Condition 1.
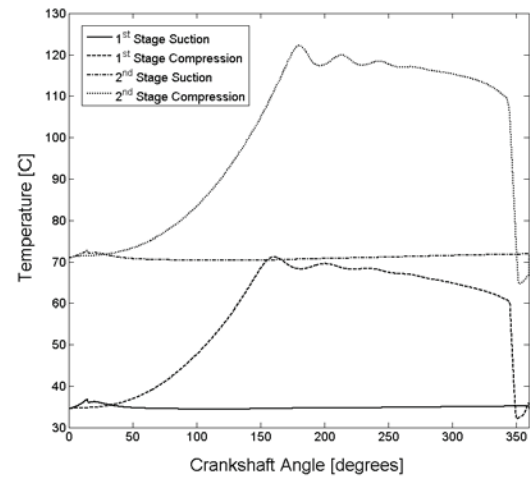
Figure 5. Variation of temperature with crankshaft angle predicted at Test Condition 1.

the shell to the first stage and the heat transfer to the first stage depends on the shell temperature, the calculations must now be repeated with the updated discharge temperature. When the discharge temperature converges, the muffler pressure is updated to attempt to satisfy an overall mass balance. The first stage muffler pressure is adjusted until the mass flow rate through the two stages agrees within the specified tolerance. Figure 3 provides a flowchart of the program showing the iterative process.

4. RESULTS AND DISCUSSION

4.1 Model Results
The model was tuned to accurately predict discharge temperature, mass flow rate, and power consumption based on the external measurements taken at test conditions similar to those encountered in air conditioning applications. "Test Condition 1" is used to reference an evaporating temperature of 10.1°C, a suction gas temperature of 33.5°C, and a condensing temperature of 55.3°C for the remainder of this paper. The parameters that were tuned included the damping coefficients of the valve model, the combined motor and mechanical efficiency, the friction coefficient for the largest leakage path, m_{32}, and the heat transfer coefficient between the compressor and the surroundings. While tuning these parameters improved the model's accuracy, a sensitivity study was also performed to demonstrate that the isentropic and volumetric efficiencies were not highly dependent on these parameters. The only exception was the combined motor-mechanical efficiency, to which the isentropic efficiency was nearly proportional.

The variation of pressure with crankshaft angle in the suction and compression chambers predicted by the tuned model is shown in Figure 4. The results are plotted with the beginning of the compression process for each stage shown as 0°. However, it is important to remember that the two stages operate 180° out of phase. The variation of temperature with crankshaft angle for the same compressor at the same operating conditions is shown in Figure 5.

The model reveals that leakage has a significant impact on compressor performance. A study of the total mass flow rate through each path in the first stage over an entire revolution shows that the most significant source of leakage is through the contact between the roller and cylinder wall, m_{32}.

Table 1. Model Results at Test Condition 1 with and without Intercooling to Maintain a 10ºC Superheat

	Without Intercooling	With Intercooling
Intermediate Pressure, kPa	1745	1463
Intermediate Temperature, ºC	69.2	69.4
Discharge Temperature, ºC	112.8	89.7
Power Consumption, kW	2.08	1.89
Mass Flow Rate, kg/hr	133.4	133.9
Isentropic Efficiency		
First Stage	64.8%	59.4%
Second Stage	69.3%	68.2%
Volumetric Efficiency		
First Stage	95.4%	96.2%
Second Stage	94.6%	94.9%

The leakages across the top and bottom of the vane, m_{vb}, are also significant. By summing the mass flow rate through all of the leakage paths it can be seen that the leakage accounts for about 3.95% of the total mass flow rate.

When intercooling is incorporated, the mass flow rate through the first stage does not change significantly because the first stage suction state has not changed. Therefore, the mass flow rate through the second stage and thus, the density of the gas entering the second stage, should not change significantly when intercooling is incorporated. To achieve the same gas density at the second stage suction when the intermediate temperature is lower due to intercooling, the intermediate pressure becomes lower. The main benefit of intercooling is reduced power consumption, which is summarized in Table 1 by comparing the cases with and without intercooling. There is almost a 10% reduction in power requirement for intercooling at these conditions. The primary improvement results from increased density of the suction gas for the second stage that leads to lower isentropic work along with an improvement in the volumetric efficiencies.

4.2 Comparison of Model and Experimental Results

The model was validated by testing a prototype compressor on a load stand at seventeen different operating conditions. A detailed description of the load stand can be found in the paper by Chen *et al.* (2002b) that documents experimental testing of a scroll compressor. Table 2 compares the model results at Test Condition 1 without intercooling to the experimental results. Because the power required for each stage of compression was not measured experimentally, the actual power consumption term in the isentropic efficiency calculation had to be estimated as the product of mass flow rate and enthalpy change. This resulted in a slightly different modeled isentropic efficiency compared to the values in Table 1. However, the tuned model predictions agree well with the experimental results.

For the majority of the cases the discharge temperatures are predicted within ±10ºC of the measured values, as shown in Figure 6. The error in the discharge temperature would partially result from the error in the intermediate temperature predicted by the model. However, uncertainty in the calculation of heat lost by natural convection from the shell would also contribute to this error.

Figure 7 compares the predicted and measured power consumption of the compressor. The power meter used for the experimental measurements has an accuracy of ±0.2%, so the error bars for the experimental points are not visible in this case. All of the model results agree with the experimental results within ±5%, but the model seems to be most accurate for cases with high power consumption. This could indicate that the constant combined mechanical and motor efficiency of 78.3% that the model assumes is more accurate for the higher power consumption cases. The motor may operate less efficiently in the cases corresponding to lower torques.

The mass flow rate through the compressor predicted by the model is also predicted within ±5% of the experimental values, as shown in Figure 8. The accuracy of the mass flow measurement depends on the mass flow rate, but the

Table 2. Summary of Model Results at Test Condition 1 Compared to Experimental Results

	Modeled	Experimental	Uncertainty in Experimental Measurement	Error in Modeled Result Compared to Experimental Result
Intermediate Pressure, kPa	1745	1780	±1%	2.0%
Intermediate Temperature, ºC	69.2	70.9	±2.2ºC	1.7 ºC
Discharge Temperature, ºC	112.8	111.2	±2.2ºC	1.6°C
Power Consumption, kW	2.08	2.08	±0.2%	0.02%
Mass Flow Rate, kg/hr	133.4	133.2	±0.7%	0.18%
Isentropic Efficiency				
First Stage	51.4%	51.0%	±6.7%	0.8%
Second Stage	76.8%	84.2%	±12.5%	9.6%
Volumetric Efficiency				
First Stage	95.4%	95.0%	±1.8%	0.4%
Second Stage	94.6%	92.9%	±1.4%	1.8%
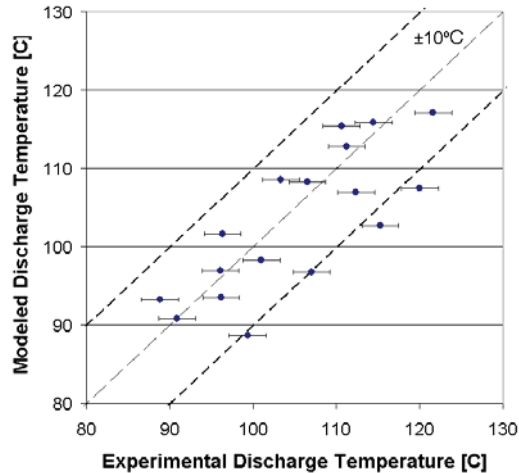
Figure 6. Comparison of predicted and measured discharge temperatures.
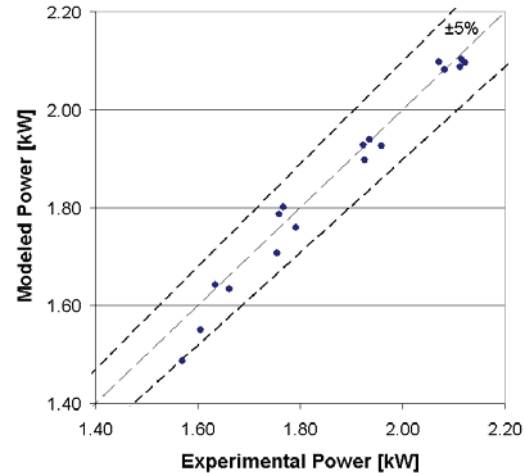
Figure 7. Comparison of predicted and measured power consumption.

accuracy is at least ±0.9% for all of the cases shown. The modeled flow rate is generally over-predicted at lower mass flow rates, which correspond to cases with the largest ratio between discharge and suction pressure. This indicates that the leakage is slightly under-predicted by the model for these cases.

Finally, Figure 9 shows that there is good agreement between the energy efficiency ratio, EER, calculated from the model and experimental results. The EER was calculated assuming that a vapor-compression cycle operates with 5 K of subcooling exiting the condenser. Employing an uncertainty analysis proposed by Begeš *et al.* (2002), the accuracy of the experimental EER is within ±0.8%.

In summary, the model accurately predicts the mass flow rate through the compressor and its power consumption. However, there is a wider range of error in the predicted intermediate and discharge temperatures, and the intermediate pressure. This is to be expected as a result of tuning the model using only one particular set of experimental results at one test condition.

5. CONCLUSIONS

The agreement between external measurements and model results suggests that the model provides a good estimate of compressor performance (within 5% for mass flow rate and power). The model not only predicts the pressure and
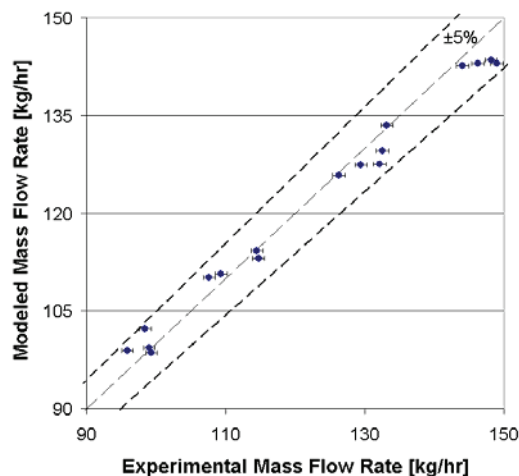
Figure 8. Comparison of predicted and measured mass flow rates.
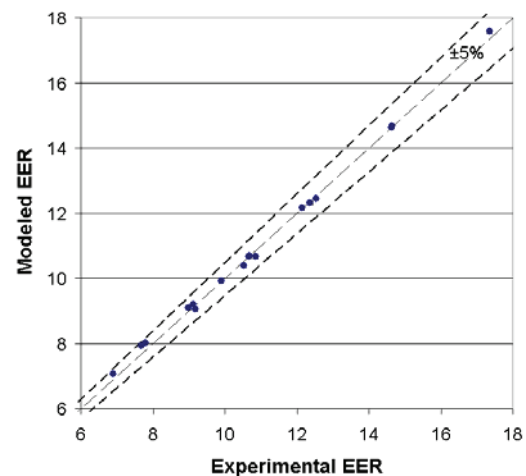
Figure 9. Comparison of EER for experimental and modeled results.

temperature distributions in the suction and compression chambers, but also provides estimates of the mass flow rates through the various leakage paths and the heat transfer from the cylinder walls. Therefore, the effect of leakage and heat transfer on the performance of the compressor can be determined. The model was used to study the performance of an existing compressor prototype with and without intercooling. For a single case, intercooling resulted in an approximately 10% improvement in compressor EER.

NOMENCLATURE

e	Eccentricity of roller	(m)		u	Specific internal energy	(J/kg)
E_{cv}	Total energy in the control volume	(J)		V	Volume	(m^3)
h	Specific enthalpy	(J/kg)		$\dot{W}$	Power	(W)
h_c	Convective heat transfer coefficient	(W/m^2·K)				
k	Thermal conductivity	(W/m·K)		Greek Symbols		
$\dot{m}$	Mass flow rate	(kg/s)		δ	Distance between the cylinder wall	
P	Pressure	(Pa)			and roller	(m)
$\dot{Q}$	Heat transfer rate	(W)		θ	Crankshaft angle	(deg)
R_c	Cylinder radius	(m)		ρ	Density	(kg/m^3)
R_r	Roller radius	(m)		φ	Angle at which distance δ is measured	(deg)
t	Time	(s)		ω	Rotational speed of crankshaft	(deg/s)
T	Temperature	(C)				

REFERENCES

Begeš, G., Drnovšek, J., Pušnik, I., Bojkovski, J., 2002, Calculation and proper presentation of the measurement uncertainty in testing, *Proc. IEEE Instrum. Meas. Technol. Conf.,* IEEE: p. 1457-1460.

Chen, Y., Halm, N.P., Groll, E.A., Braun, J.E., 2002a, Mathematical modeling of scroll compressors—Part I: Compression process modeling, *Int. J. Refrig.*, vol. 25, no. 6: p. 731-750.

Chen, Y., Halm, N.P., Braun, J.E., Groll, E.A., 2002b, Mathematical modeling of scroll compressors—Part II: Overall scroll compressor modeling, *Int. J. Refrig.*, vol. 25, no. 6: p. 751-764.

Jun, Y., 2002, Mechanical loss analysis of inverter controlled two cylinders type rotary compressor, *Proc. Int. Compres. Eng. Conf. at Purdue*, C5-6.

Lee, J., Min, T.S., 1988, Performance analysis of rolling piston type rotary compressor, *Proc. Int. Compres. Eng. Conf. at Purdue*, p. 154-162.

Munson, B.R., Young, D.F., Okiishi, T.H., 2002, *Fundamentals of fluid mechanics*, Wiley, New York, 840 p.

Okada, K., Kuyama, K., 1982, Motion of rolling piston in rotary compressor, *Proc. Int. Compres. Eng. Conf. at Purdue*, p. 178-184.

Padhy, S.K., Dwivedi, S.N., 1994, Heat transfer analysis of a rolling-piston rotary compressor, *Int. J. Refrig.*, vol. 17, no. 6: p. 400-410.

Shimizu, T., Kobayashi, M., Yanagisawa, T., 1980, Volumetric efficiency and experimental errors of rotary compressors, *Int. J. Refrig.*, vol. 3, no. 4: p. 219-225.

Yanagisawa, T., Shimizu, T., Chu, I., Ishijima, K., 1982, Motion analysis of rolling piston in rotary compressor, *Proc. Int. Compres. Eng. Conf. at Purdue*, p. 185-192.

Yanagisawa, T., Shimizu, T., 1985a, Leakage losses with a rolling piston type rotary compressor. I. Radial clearance on the rolling piston, *Int. J. Refrig.*, vol. 8, no. 2: p. 75-84.

Yanagisawa, T., Shimizu, T., 1985b, Leakage losses with a rolling piston type rotary compressor. II. Leakage losses through clearances on rolling piston faces, *Int. J. Refrig.*, vol. 8, no. 3: p. 152-158.

Yi, F., Groll, E.A., Braun, J.E., 2004, Modeling and testing of an automobile AC scroll compressor, part I: Model development, *Proc. Int. Compres. Eng. Conf. at Purdue*, C082.

ACKNOWLEDGEMENT